



Performance analysis of decode-and-forward partial relay selection in NOMA systems with RF energy harvesting

Tran Manh Hoang¹ · Nguyen Trung Tan¹ · Nguyen Huy Hoang¹ · Pham Thanh Hiep¹ 

Published online: 16 May 2018
© Springer Science+Business Media, LLC, part of Springer Nature 2018

Abstract

In this paper, we investigate a dual hop communication decode-and-forward scheme relay system where a source node wants to transmit simultaneously two symbols to two desired destinations with the help of one selected energy constraint relay node. The power for operation of relay is come from the ambient radio frequency energy harvesting and the non-orthogonal multiple access technology is applied. We mathematically evaluate the impact of partial relay selection on the system performance by considering the undecodable probability of symbol for which symbols can not be decoded at the relay node or two destinations. Furthermore, the undecodable probability and the ergodic capacity are analyzed under the effect of imperfect and perfect successive interference cancellation (SIC). The results of theoretical analysis is similar to the simulation results, especially in the high region of transmit power. It verifies the correctness of mathematical closed-form in our analysis. The results also show that the performance of the system are significantly influenced by the efficiency of SIC technology and the number of relay nodes.

Keywords NOMA · Partial relay section · Energy harvesting · Perfect and imperfect successive interference cancellation

1 Introduction

Non-orthogonal multiple access (NOMA) has been proven as a promising technique for the fifth generation (5G) mobile networks due to its superior spectral efficiency [1]. Unlike orthogonal-multiple-access (OMA), NOMA allows multiple users to pair and share the same radio resources, either in time, frequency or in code. The key idea of NOMA is to explore power domain, where users are served at different power levels [2]. More importantly, NOMA has recently been recognized as a promising multiple access (MA) technique to significantly improve the spectral efficiency of mobile communication networks. It is also been

envisioned as a key component in fifth generation (5G) mobile systems, it has also been applied to cooperative relay systems [3, 4]. In [3], the cooperative NOMA system with buffer-aided relaying was studied. Assuming that the relay node possesses a buffer, the authors proposed an adaptive transmission scheme in which the system adaptively chooses its working mode in each time slot. The authors in [4] proposed and investigated a dual-hop cooperative relaying scheme using NOMA, where two sources communicate with their corresponding destinations simultaneously over the same frequency band and via a common relay. After receiving symbols transmitted from both sources with different allocated powers, the relay forwards a superposition coded composite signal to the destinations by using NOMA technique.

On the other hand, despite of advantages of simultaneous wireless information and power transfer (SWIPT), the research on it is lack, especially studying of join of SWIPT and NOMA relay systems. There are several researches on NOMA systems combining radio frequency (RF) energy harvesting (EH) as follows. The general combination of NOMA and EH was investigated in [5–7]. SWIPT of NOMA networks where users are spatially randomly located,

✉ Pham Thanh Hiep
phamthanhhiiep@gmail.com

Tran Manh Hoang
tranmanhhoang@tcu.edu.vn

Nguyen Trung Tan
trungtan68@gmail.com

Nguyen Huy Hoang
hoangnh@mta.edu.vn

¹ Le Quy Don Technical University, Hanoi, Vietnam

was also investigated [8]. The system in which the users closer to the source act as EH relays to help the users farther was analyzed. The outage performance of NOMA-EH relaying networks with antenna selection at the source and splitting power at the relay was discussed in [7]. To the best of our knowledge, the aforementioned work, the EH on the partial relay selection (PRS) combining with NOMA technique, has not been discussed. Therefore, we decide the main contributions of this paper are as follows:

- We propose a NOMA system where the relay node harvests energy from the radio frequency by using time switching scheme to support the operation of forwarding information to both of users.
- In order to evaluate the performance of partial selection relay scheme, we derive closed-form expressions of undecodable probability and ergodic capacity. Undecodable probability is defined as probability the desired information at the best relay node and/or the destination nodes can not be decoded successfully because of low signal to noise ratio (SNR).
- The performance of NOMA-EH system under the imperfect SIC and perfect SIC is analyzed and compared with each other and with the orthogonal frequency division multiple access (OFDMA).
- According to the channel gains, the detailed power allocation coefficient for is settled for fairness in performance of users

The rest of this paper is organized as follows Sect. 2 describes the system model of partial relay selection in NOMA system with RF EH. The mathematical analysis of the system is represented in Sect. 3. Numerical results are shown in Sect. 4 to examine the performance of our proposed system. Finally, the paper is concluded in Sect. 5.

2 System model

We consider a NOMA downlink system consisted of one source (S), two users (D₁ and D₂) as shown in Fig. 1. The source transmits the signal to the users via several relay nodes R_n with $n \in \{1, \dots, N\}$ which are equipped one antenna and operate in a half-duplex mode. In this paper, we only consider the case of partial relay selection. Moreover, all relays have no fixed power supply and are powered by wireless energy transfer from the source. The channels from the S to R_n and from R_n to D_i with $i \in \{1, 2\}$, exhibit frequency, flat Rayleigh block fading.

As shown in Fig. 1, $h_{1,n} \sim \mathcal{CN}(0, \Omega_{1,n})$ is the complex channel coefficient between the S and R_n. $w_R, w_{D_i} \sim \mathcal{CN}(0, 1)$ are the additive white Gaussian noise (AWGN) at R_n and D_i, respectively. $g_i \sim \mathcal{CN}(0, \Omega_{R_n D_i})$

denotes the complex channel coefficient between R_n and D_i. Since the path loss and shadowing effect of g_1 are more severe than g_2 , we have $\Omega_{R_n D_1} < \Omega_{R_n D_2}$ which is important for performing the successive interference cancellation (SIC) [10]. *The relay and the user respectively receive the signal from the source and the best relay, hence the channel state information (CSI) between the source and the relay is available at the relay, the CSI between the best relay and the user is available at the user.*

In this paper, we consider the PRS scheme where relay node is selected based only on the instantaneous knowledge of the channel pertaining to the first hop. The source terminal continuously monitors the quality of its connectivity with the relays via the transmission of local feedbacks. From this information, the source selects the best link S → R_n for data transmission. As multiple relay nodes form a group, one best relay R_b is selected before transmitting. This PRS strategy is expressed as¹

$$b = \arg \max_{n=1, 2, \dots, N} |h_{1,n}|^2. \tag{1}$$

We assume that the harvested power is consumed by the relays for forwarding signals to D₁ and D₂. The processing power required for the transmitting - receiving circuitry of relay is generally negligible compared to the power used for signal transmission. The time switching (TS) architecture for EH [11]² is applied. Specifically, the energy is harvested from the received information signal for a duration of αT in each block, where α is the fraction of the block time in which the relay harvests energy from the received information signal, and T is the block time in which a certain information is transmitted from the source to the users. Hence, the harvested energy is given by [12].

$$E_h = \alpha T \eta P_S |h_{1,b}|^2, \tag{2}$$

where η is the energy conversion efficiency, depends on the quality of energy harvesting electric circuitry, $0 < \eta \leq 1$, and P_S is transmission power of S.

We assume that the duration time for relay to receive the signal from the source and to transmit the received signal to both of users is the same and equals $(1 - \alpha)T/2$. From (2), the transmission power of relay node is calculated as

$$P_R = \frac{E_h}{(1 - \alpha)T/2} = \frac{2\alpha\eta P_S |h_{1,b}|^2}{1 - \alpha}. \tag{3}$$

The operation on the system is briefly described as follows. There are two time slots involving in each transmission block. All blocks are normalized to one unit.

¹ The sequence of X are referred to as order statistics of the sequence of X_{1,n}.

² The proposed analysis approach can be applied for the power spitting EH model.

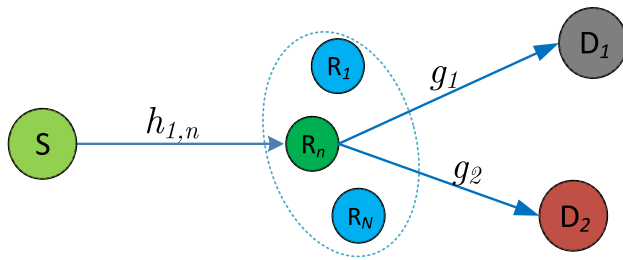


Fig. 1 Partial relaying selection in NOMA downlink relay network with RF EH

During the first time slot, the source node transmits the superimposed mixture, $\sqrt{a_1}x_1 + \sqrt{a_2}x_2$, where x_i and a_i denote the signal and the power allocation coefficient of user i , respectively. It should be noted that $a_1 + a_2 = 1$, and *without loss of generality, we assume that $a_1 \geq a_2$* [13]. The baseband received signal at R_n is thus given by

$$y_R^n = \sqrt{P_S}h_{1,n}(\sqrt{a_1}x_1 + \sqrt{a_2}x_2) + w_R. \tag{4}$$

Since the key idea of NOMA technique is to use the power domain for multiple accesses, i.e. users are served at different power levels, and to adopt the superposition code at the transmitter. We use the SIC principle to decode signals at the receivers, such as the stronger signal is decoded and removed from the superposed signals, and then the weaker signal is decoded to obtain the desired information. Thus, in this paper, we only consider SIC process at the best relay node and the D_2 because the D_1 , which is allocated higher transmit power, decodes the superimposed mixture signal and obtains its own signal while considering the other signal as noise.

When the SIC is employed at the R_n , the best relay, R_b , firstly decodes symbol x_1 by treating the symbol x_2 as noise. Then, it performs SIC to obtain symbol x_2 . Thus, the received signal-to-interference-plus-noise ratio (SINR) for symbol x_1 and signal-to-noise ratio (SNR) for symbol x_2 at R_b are written as

$$\gamma_{1u_1} = \frac{a_1 P_S |h_{1,b}|^2}{a_2 P_S |h_{1,b}|^2 + 1}, \tag{5}$$

$$\gamma_{1u_2} = a_2 P_S |h_{1,b}|^2. \tag{6}$$

In the first time slot, R_n processes messages x_1, x_2 and in the second time slot, the selected relay sends the message $\sqrt{P_R}(\sqrt{a_1}x_1 + \sqrt{a_2}x_2)$ to two users D_1 and D_2 . Hence, the received signal at D_i is described as follows.

$$y_{D_i} = \sqrt{P_R}g_i(\sqrt{a_1}x_1 + \sqrt{a_2}x_2) + w_{D_i}, \tag{7}$$

where g_i denotes the channel gain between the selected relay and D_i .

According to the SIC principle, the D_1 decodes symbol x_1 while treating x_2 as noise. From (7), the signal-to-interference-plus-noise ratio (SINR) at D_1 is given by

$$\gamma_{2u_1} = \frac{a_1 P_R |g_1|^2}{a_2 P_R |g_1|^2 + 1}. \tag{8}$$

It should be noticed that x_1 and x_2 coexist at D_2 . Therefore, the SIC is needed to decode own symbol x_2 . To perform SIC, D_2 decodes high-power symbol x_1 by treating the low-power symbol x_2 as noise, and cancels it using SIC to obtain symbol x_2 . Thus, the received SINR for x_1 at D_2 is given by

$$\gamma_{2u_1 \rightarrow u_2} = \frac{a_1 P_R |g_2|^2}{a_2 P_R |g_2|^2 + 1}. \tag{9}$$

After cancelling x_1 , D_2 decodes its own message, x_2 , with the SNR as

$$\gamma_{2u_2} = a_2 P_R |g_2|^2. \tag{10}$$

3 Performance analysis

In this section, we discuss on undecodable probability and ergodic capacity of partial relay selection scheme NOMA system with RF EH. The undecodable probability can be referred as the probability that symbols x_1 and x_2 are not able to be decoded at D_1 and D_2 . In additional, a symbol is not able to be decoded if the received SNR or SINR is lower than the threshold value, γ .

3.1 Undecodable probability of x_1

We denote $P_{x_1}^{\text{error}}$ as the event that the best relay or D_1 or D_2 cannot decode x_1 successfully because the SINR/SNR is lower than the threshold value, $\gamma_{\text{th}1}$. From (5), (8), and (9), we can write the expression of $P_{x_1}^{\text{error}}$ as in (11) [14],

$$\begin{aligned}
 P_{x_1}^{\text{error}} &= \Pr \left\{ \begin{aligned} &\frac{a_1 P_S |h_{1,b}|^2}{a_2 P_S |h_{1,b}|^2 + 1} < \gamma_{\text{th}1}, \\ &\text{or } \frac{a_1 P_R |g_1|^2}{a_2 P_R |g_1|^2 + 1} < \gamma_{\text{th}1}, \\ &\text{or } \frac{a_1 P_R |g_2|^2}{a_2 P_R |g_2|^2 + 1} < \gamma_{\text{th}1} \end{aligned} \right\} \\
 &= 1 - \Pr \left\{ \begin{aligned} &\frac{a_1 P_S |h_{1,b}|^2}{a_2 P_S |h_{1,b}|^2 + 1} > \gamma_{\text{th}1}, \\ &\frac{a_1 P_R |g_1|^2}{a_2 P_R |g_1|^2 + 1} > \gamma_{\text{th}1}, \\ &\frac{a_1 P_R |g_2|^2}{a_2 P_R |g_2|^2 + 1} > \gamma_{\text{th}1} \end{aligned} \right\}, \tag{11}
 \end{aligned}$$

where $\gamma_{\text{th}1} = 2^{\frac{2r_1}{1-\alpha}} - 1$ and r_1 is the target data rate of D_1 . Let $|h_{1,b}|^2 = X$, $|g_1|^2 = Y$, and $|g_2|^2 = Z$ be the channel gains from the source to the best relay and from the best relay to D_1 and D_2 , respectively. In this paper, we assume that all channel coefficients are modeled as independent Rayleigh-distributed random variables (RVs). Therefore, RVs $|h_{1,b}|^2$, $|g_1|^2$, and $|g_2|^2$ have exponential distributions, with

$$\begin{aligned}
 f_X(x) &= \sum_{n=1}^N (-1)^{n-1} \binom{N}{n} \frac{n}{\Omega_1} \exp\left(-\frac{nx}{\Omega_1}\right), \\
 f_Y(y) &= \frac{1}{\Omega_2} \exp\left(-\frac{y}{\Omega_2}\right), F_Y(y) = 1 - \exp\left(-\frac{y}{\Omega_2}\right), \\
 f_Z(z) &= \frac{1}{\Omega_3} \exp\left(-\frac{z}{\Omega_3}\right).
 \end{aligned}$$

where f and F are respectively the cumulative density function and probability density function, $\Omega_1 = \mathbb{E}\{|h_{1,b}|^2\}$, $\Omega_2 = \mathbb{E}\{|g_1|^2\}$ and $\Omega_3 = \mathbb{E}\{|g_2|^2\}$ are means of random variables. We can rewrite (11) to become (12)

$$P_{x_1}^{\text{error}} = 1 - \Pr \left\{ \begin{aligned} &X > \frac{\gamma_{\text{th}1}}{P_S(a_1 - a_2\gamma_{\text{th}1})} \\ &XY > \frac{\gamma_{\text{th}1}}{P_S\phi(a_1 - a_2\gamma_{\text{th}1})} \\ &XZ > \frac{\gamma_{\text{th}1}}{P_S\phi(a_1 - a_2\gamma_{\text{th}1})} \end{aligned} \right\}, \tag{12}$$

where $\phi = \frac{2\alpha\eta}{1-\alpha}$. As can be seen from (12), the outage always occurs if $\gamma_{\text{th}1} > \frac{a_1}{a_2}$. Hence, we need to allocate more power for symbol x_1 meaning $a_1 > a_2\gamma_{\text{th}1}$ is required. By using the conditional probability in [15], we can rewrite (12) as

$$\begin{aligned}
 P_{x_1}^{\text{error}} &= 1 - \int_{t_1}^{\infty} \Pr\left\{Y > \frac{t_2}{x}, Z > \frac{t_2}{x}\right\} f_X(x) dx \\
 &= 1 - \int_{t_1}^{\infty} \int_{\frac{t_2}{x}}^{\infty} [1 - F_Y\left(\frac{t_2}{x}\right)] f_Z(z) f_X(x) dx dz, \tag{13}
 \end{aligned}$$

where

$$t_1 = \frac{\gamma_{\text{th}1}}{P_S(a_1 - a_2\gamma_{\text{th}1})} \quad \text{and} \quad t_2 = \frac{\gamma_{\text{th}1}}{P_S\phi(a_1 - a_2\gamma_{\text{th}1})}.$$

From (13) and after some manipulation, we have

$$P_{x_1}^{\text{error}} = 1 - \sum_{n=1}^N (-1)^{n-1} \binom{N}{n} \frac{n}{\Omega_1} \underbrace{\int_{t_1}^{\infty} \exp\left(-\frac{\beta}{x} - \frac{nx}{\Omega_1}\right) dx}_{\psi}, \tag{14}$$

where $\beta = \frac{t_2}{\Omega_2} + \frac{t_2}{\Omega_3}$. Unfortunately, a closed-form expression for ψ in (14) is difficult to be derived, thus we employ the approximation method. By using expanded Taylor’s series, it follows that $\exp\left(-\frac{a}{x}\right) = \sum_{k=0}^{N_t} \frac{(-1)^k}{k!} \left(\frac{a}{x}\right)^k$, where $N_t \in \{1, \dots, \infty\}$. Then, we obtain

$$\begin{aligned}
 \psi &= \sum_{k=0}^{N_t} \frac{(-1)^k}{k!} \int_{t_1}^{\infty} \left(\frac{\beta}{x}\right)^k \exp\left(-\frac{nx}{\Omega_1}\right) dx \\
 &= \sum_{k=0}^{N_t} \frac{(-1)^k \beta^k}{k!} \left(\frac{1}{t_1}\right)^{k-1} E_k\left(\frac{nt_1}{\Omega_1}\right), \tag{15}
 \end{aligned}$$

where $E_k(\cdot)$ is the exponential integral function [9]. Substituting (15) into (14), we get the expression of $P_{x_1}^{\text{error}}$ as

$$P_{x_1}^{\text{error}} = 1 - \sum_{n=0}^N \sum_{k=0}^{N_t} \frac{(-1)^n (-1)^k \beta^k}{k!} \binom{N}{n} \frac{n}{\Omega_1} \left(\frac{1}{t_1}\right)^{k-1} E_k\left(\frac{nt_1}{\Omega_1}\right). \tag{16}$$

As we can see from (14), if the transmit power lies in a high region, it leads to $t_1 = \frac{\gamma_{\text{th}1}}{P_S \approx \infty (a_1 - a_2\gamma_{\text{th}1})} \rightarrow 0$. Thus, we apply [9, (3.324.1)] to obtain the final expression of $P_{x_1}^{\text{error}}$ as

$$P_{x_1}^{\text{error}} \approx 1 - \sum_{n=1}^N (-1)^{n-1} \binom{N}{n} \sqrt{\frac{4n\beta}{\Omega_1}} K_1\left(\sqrt{\frac{4n\beta}{\Omega_1}}\right), \tag{17}$$

where $K_1(\cdot)$ is the first-order modified Bessel function of the second kind.

3.2 Undecodable probability of x_2

In this paper, we consider two scenarios, the first scenario is perfect SIC, and the second one is imperfect SIC at both R_b and D_2 .

3.2.1 In case of perfect SIC

In this NOMA system, the SIC technique is carried out at D_2 to remove signal x_1 before detecting its own message. In case SIC is perfect at D_2 and $P_{x_2}^{\text{error}}$ is denoted as the event that the best relay or D_2 cannot correctly decode symbol x_2 because the SNR is lower than the threshold value, $\gamma_{\text{th}2} = 2^{\frac{r_2}{1-\alpha}} - 1$ where r_2 is the target data rate of D_2 . Then, the expression of $P_{x_2}^{\text{error}}$ is given by

$$P_{x_2}^{\text{error}} = \Pr(\min(\gamma_{1u_2}, \gamma_{2u_2}) \leq \gamma_{\text{th}2}) = 1 - \Pr(a_2 P_S |h_{1,b}|^2 > \gamma_{\text{th}2}, a_2 P_R |g_2|^2 > \gamma_{\text{th}2}). \tag{18}$$

Substituting P_R from (3) into (18), we can rewrite as

$$P_{x_2}^{\text{error}} = 1 - \Pr\left(X > \frac{\gamma_{\text{th}2}}{a_2 P_S}, Z > \frac{\gamma_{\text{th}2}(1-\alpha)}{X 2 a_2 \alpha \eta P_S}\right). \tag{19}$$

Based on the conditional probability [15], we can express (19) as

$$P_{x_2}^{\text{error}} = 1 - \int_a^\infty \left[1 - F_Z\left(\frac{b}{x}\right)\right] f_X(x) dx, \tag{20}$$

where $a = \frac{\gamma_{\text{th}2}}{a_2 P_S}$ and $b = \frac{\gamma_{\text{th}2}(1-\alpha)}{2 a_2 \alpha \eta P_S}$. By substituting the cumulative distribution functions (CDF) and probability density function (PDF) of X and Y into (20) and then using expanded Taylor series, we obtain the expression of $P_{x_2}^{\text{error}}$ as in (21).

$$P_{x_2}^{\text{error}} = 1 - \sum_{n=1}^N (-1)^{n-1} \binom{N}{n} \frac{n}{\Omega_1} \int_a^\infty \exp\left(-\frac{b}{\Omega_3 x}\right) \exp\left(-\frac{nx}{\Omega_1}\right) dx = 1 - \sum_{n=1}^N (-1)^{n-1} \binom{N}{n} \frac{n}{\Omega_1} \sum_{k=0}^{N_n} \frac{(-1)^k}{k!} \left(\frac{b}{\Omega_3}\right)^k \left(\frac{1}{a}\right)^{k-1} E_k\left(\frac{na}{\Omega_1}\right). \tag{21}$$

Similar to undecodable probability of x_1 , when the transmit power lies in a high region, it will lead to $a = \frac{\gamma_{\text{th}2}}{a_2 P_S} \rightarrow 0$. Hence, the approximate expression of $P_{x_2}^{\text{error}}$ is given by

$$P_{x_2}^{\text{error}} \approx 1 - \sum_{n=1}^N (-1)^{n-1} \binom{N}{n} \sqrt{\frac{4bn}{\Omega_1 \Omega_3}} K_1\left(\sqrt{\frac{4bn}{\Omega_1 \Omega_3}}\right). \tag{22}$$

3.2.2 In case of imperfect SIC

In this scenario, the symbol x_1 is incompletely removed and becomes the interference. The SINRs of symbol x_2 at R_b and D_2 are respectively given as

$$\gamma_{1u_2} = \frac{a_2 P_S |h_{1,b}|^2}{a_1 \rho_1 P_S |h_{1,b}|^2 + 1}, \tag{23}$$

$$\gamma_{2u_2} = \frac{a_2 P_R |g_2|^2}{a_1 \rho_2 P_R |g_2|^2 + 1}, \tag{24}$$

where $0 \leq \rho_i \leq 1$ with $i \in \{1, 2\}$ denotes the level of residual interference due to the imperfect SIC at R_b and D_2 . Especially, $\rho_i = 1$ and $\rho_i = 0$ refer to the cases of without SIC and perfect SIC, respectively. From (23) and (24), we have the undecodable probability of x_2 for the case of imperfect SIC shown in (25).

$$P_{x_2}^{\text{ISIC}} = \Pr\left[\min\left(\frac{a_2 P_S |h_{1,b}|^2}{a_1 P_S \rho_1 |h_{1,b}|^2 + 1}, \frac{a_2 P_R |g_2|^2}{a_1 P_R \rho_2 |g_2|^2 + 1}\right) \leq \gamma_{\text{th}2}\right]. \tag{25}$$

After solving (25), we get the result as

$$P_{x_2}^{\text{ISIC}} = 1 - \int_c^\infty \left[1 - F_Z\left(\frac{d}{x}\right)\right] f_X(x) dx, \tag{26}$$

where

$$c = \frac{\gamma_{\text{th}2}}{P_S(a_2 - a_1 \rho_1 \gamma_{\text{th}2})}, \quad d = \frac{\gamma_{\text{th}2}}{\phi P_S(a_2 - a_1 \rho_2 \gamma_{\text{th}2})}.$$

Then, with some further manipulations, we can rewrite (26) into (27).

$$P_{x_2}^{\text{ISIC}} = 1 - \sum_{n=1}^N (-1)^{n-1} \binom{N}{n} \frac{n}{\Omega_1} \int_c^\infty \exp\left(-\frac{d}{\Omega_3 x}\right) \exp\left(-\frac{nx}{\Omega_1}\right) dx = 1 - \sum_{n=1}^N (-1)^{n-1} \binom{N}{n} \frac{n}{\Omega_1} \sum_{k=0}^{N_n} \frac{(-1)^k}{k!} \left(\frac{d}{\Omega_3}\right)^k \left(\frac{1}{c}\right)^{k-1} E_k\left(\frac{nc}{\Omega_1}\right). \tag{27}$$

In high-power region, we have the approximate expression of $P_{x_2}^{\text{ISIC}}$ as

$$P_{x_2}^{\text{ISIC}} \approx 1 - \sum_{n=1}^N (-1)^{n-1} \binom{N}{n} \sqrt{\frac{4nd}{\Omega_1 \Omega_3}} K_1\left(\sqrt{\frac{4nd}{\Omega_1 \Omega_3}}\right). \tag{28}$$

3.3 Ergodic capacity

3.3.1 In case of perfect SIC

In this section, we investigate the ergodic capacity of the system, the achievable sum rate of the NOMA downlink is given as

$$\bar{C}_{sum} = \bar{C}_{D_1}^{x_1} + \bar{C}_{D_2}^{x_2}. \tag{29}$$

The achievable capacity at the D₁ is given as

$$\begin{aligned} C_{D_1}^{x_1} &= \frac{1-\alpha}{2} \log_2(1 + \min\{\gamma_{1u_1}, \gamma_{2u_1}\}) \\ &= \frac{1-\alpha}{2} \log_2\left(1 + \min\left\{\frac{a_1 P_S |h_{1,b}|^2}{a_2 P_S |h_{1,b}|^2 + 1}, \frac{a_1 P_R |g_1|^2}{a_2 P_R |g_1|^2 + 1}\right\}\right). \end{aligned} \tag{30}$$

In practice, the amount of harvested energy at the relay is always small, hence the transmit power of relay is much lower than that of the source, and then the assumption that SINR at the destinations is lower than the SINR at the relay is reasonable.

$$\frac{a_1 P_S |h_{1,b}|^2}{a_2 P_S |h_{1,b}|^2 + 1} > \frac{a_1 P_R |g_1|^2}{a_2 P_R |g_1|^2 + 1}.$$

Hence, from (30) we have

$$\begin{aligned} C_{D_1}^{x_1} &= \frac{1-\alpha}{2} \log_2\left(1 + \frac{P_R |g_1|^2 a_1}{P_R |g_1|^2 a_2 + 1}\right) \\ &= \frac{1-\alpha}{2} \log_2\left(\frac{\phi P_S |h_{1,b}|^2 |g_1|^2 + 1}{\phi P_S |h_{1,b}|^2 |g_1|^2 a_2 + 1}\right). \end{aligned} \tag{31}$$

With the instantaneous capacity is derived in (31), we obtain the ergodic capacity of the D₁ as

$$\begin{aligned} \bar{C}_{D_1}^{x_1} &= \mathbb{E}\left\{\frac{1-\alpha}{2} \log_2\left(1 + \phi P_S |h_{1,b}|^2 |g_1|^2\right)\right\} \\ &\quad - \mathbb{E}\left\{\frac{1-\alpha}{2} \log_2\left(1 + a_2 \phi P_S |h_{1,b}|^2 |g_1|^2\right)\right\} \\ &= \underbrace{\frac{1-\alpha}{2 \ln 2} \int_0^\infty \frac{1-F_Q(\xi)}{1+\xi} d\xi}_{I_1} - \underbrace{\frac{1-\alpha}{2 \ln 2} \int_0^\infty \frac{1-F_P(\xi)}{1+\xi} d\xi}_{I_2}, \end{aligned} \tag{32}$$

where $Q = \phi P_S |h_{1,b}|^2 |g_1|^2$ and $P = a_2 \phi P_S |h_{1,b}|^2 |g_1|^2$. Based on the condition probability we have the CDFs of Q and P , respectively.

$$F_Q(\xi) = 1 - \sum_{n=1}^N (-1)^{n-1} \binom{N}{n} \sqrt{\frac{4n\xi}{\phi P_S \Omega_1 \Omega_2}} K_1\left(\sqrt{\frac{4n\xi}{\phi P_S \Omega_1 \Omega_2}}\right). \tag{33}$$

$$F_P(\xi) = 1 - \sum_{n=1}^N (-1)^{n-1} \binom{N}{n} \sqrt{\frac{4n\xi}{a_2 \phi P_S \Omega_1 \Omega_2}} K_1\left(\sqrt{\frac{4n\xi}{a_2 \phi P_S \Omega_1 \Omega_2}}\right). \tag{34}$$

With the help of the [9, eq. (7.811.5), (9.34.3)] and after some manipulation we have.

$$I_1 = \frac{1-\alpha}{2 \ln 2} \sum_{n=1}^N (-1)^{n-1} \binom{N}{n} G_{13}^{31}\left(\frac{n}{\phi P_S \Omega_1 \Omega_2} \middle| 0_{0, \frac{3}{4}, -\frac{1}{4}}\right). \tag{35}$$

$$I_2 = \frac{1-\alpha}{2 \ln 2} \sum_{n=1}^N (-1)^{n-1} \binom{N}{n} G_{13}^{31}\left(\frac{n}{a_2 \phi P_S \Omega_1 \Omega_2} \middle| 0_{0, \frac{3}{4}, -\frac{1}{4}}\right). \tag{36}$$

The achievable capacity at the D₂ is given as

$$C_{D_2}^{x_2} = \frac{1-\alpha}{2} \log_2(1 + \min\{\gamma_{1u_2}, \gamma_{2u_2}\}). \tag{37}$$

Similarly, we get the ergodic capacity of the D₂ is given as

$$C_{D_2}^{x_2} = \frac{1-\alpha}{2 \ln 2} \sum_{n=1}^N (-1)^{n-1} \binom{N}{n} G_{13}^{31}\left(\frac{nb}{\Omega_1 \Omega_3} \middle| 0_{0, \frac{3}{4}, -\frac{1}{4}}\right). \tag{38}$$

Combining Eqs. (35), (36) and (41) we have the sum ergodic capacity of the EH-NOMA downlink relay system.

3.3.2 In case of imperfect SIC

The ergodic capacity of imperfect SIC is similar to that of perfect SIC.

$$\bar{C}_{sum}^{I-SIC} = \bar{C}_{D_1}^{x_1} + \bar{C}_{D_2}^{x_2/I-SIC}. \tag{39}$$

where the $\bar{C}_{D_1}^{x_1}$ is derived by Eqs. (30)–(36) in the above section.

The $\bar{C}_{D_2}^{x_2/I-SIC}$ can be given as

$$C_{D_2}^{x_2/I-SIC} = \frac{1-\alpha}{2} \log_2(1 + \min\{\gamma_{1,u_2}, \gamma_{2,u_2}\}), \tag{40}$$

From (23) and (24) we have

$$\begin{aligned} C_{D_2}^{x_2/I-SIC} &= \frac{1-\alpha}{2} \log_2\left[1 + \min\left(\frac{a_2 P_S |h_{1,n}|^2}{a_1 P_S \rho_1 |h_{1,n}|^2 + 1}, \frac{a_2 P_R |g_2|^2}{a_1 P_R \rho_2 |g_2|^2 + 1}\right)\right] \\ &= \frac{1-\alpha}{2} \log_2\left[1 + \left(\frac{a_2 P_R |g_2|^2}{a_1 P_R \rho_2 |g_2|^2 + 1}\right)\right]. \end{aligned} \tag{41}$$

Hence, the ergodic capacity of the x_2 in case of imperfect SIC can be rewritten as

$$\bar{C}_{D_2}^{x_2/1-SIC} = \frac{1-\alpha}{2} \mathbb{E} \left[\log_2 \left(1 + P_R |g_2|^2 (a_1 \rho_2 + a_2) \right) \right] - \frac{1-\alpha}{2} \mathbb{E} \left[\log_2 \left(1 + a_1 \rho_2 P_R |g_2|^2 \right) \right] \tag{42}$$

$$\bar{C}_{D_2}^{x_2/1-SIC} = \underbrace{\frac{1-\alpha}{2 \ln 2} \int_0^\infty \frac{1-F_U(u)}{1+u} du}_{J_1} - \underbrace{\frac{1-\alpha}{2 \ln 2} \int_0^\infty \frac{1-F_V(v)}{1+v} dv}_{J_2} \tag{43}$$

where $U = \phi P_S |h_{1,n}|^2 |g_2|^2 \kappa$, and $V = a_1 \rho_2 \phi P_S |h_{1,n}|^2 |g_2|^2$ with $\kappa = a_1 \rho_2 + a_2$, $\phi = \frac{2\alpha}{1-\alpha}$.

Based on the condition probability, the CDFs of U and V is respectively represented as.

$$F_U(u) = 1 - \sum_{n=1}^N (-1)^{n-1} \binom{N}{n} \times \sqrt{\frac{4nu}{(a_1 \rho_2 + a_2) \phi P_S \Omega_1 \Omega_3}} K_1 \left(\sqrt{\frac{4nu}{(a_1 \rho_2 + a_2) \phi P_S \Omega_1 \Omega_3}} \right) \tag{44}$$

$$F_V(v) = 1 - \sum_{n=1}^N (-1)^{n-1} \binom{N}{n} \sqrt{\frac{4nv}{a_1 \rho_2 \phi P_S \Omega_1 \Omega_3}} K_1 \left(\sqrt{\frac{4nv}{a_1 \rho_2 \phi P_S \Omega_1 \Omega_3}} \right) \tag{45}$$

Replace (44) and (45) into (43) we have

$$J_1 = \frac{1-\alpha}{2 \ln 2} \sum_{n=1}^N (-1)^{n-1} \binom{N}{n} G_{13}^{31} \left(\frac{n}{(a_1 \rho_2 + a_2) \phi P_S \Omega_1 \Omega_3} \middle|_{0, \frac{3}{4}, -\frac{1}{4}}^0 \right) \tag{46}$$

$$J_2 = \frac{1-\alpha}{2 \ln 2} \sum_{n=1}^N (-1)^{n-1} \binom{N}{n} G_{13}^{31} \left(\frac{n}{a_1 \rho_2 \phi P_S \Omega_1 \Omega_3} \middle|_{0, \frac{3}{4}, -\frac{1}{4}}^0 \right) \tag{47}$$

Finally, we have the ergodic capacity of the system in imperfect SIC as

$$\bar{C}_{sum}^{I-SIC} = I_1 - I_2 + J_1 - J_2 \tag{48}$$

where I_1, I_2 is given in Eqs. (35) and (36), respectively.

3.3.3 Ergodic capacity of OFDMA

In order to compare with orthogonal frequency division multiple access (OFDMA), which is a well-known high-capacity orthogonal multiple access (OMA) technique, the ergodic capacity of OFDMA is described in this section and the calculation result is compared in the following section.

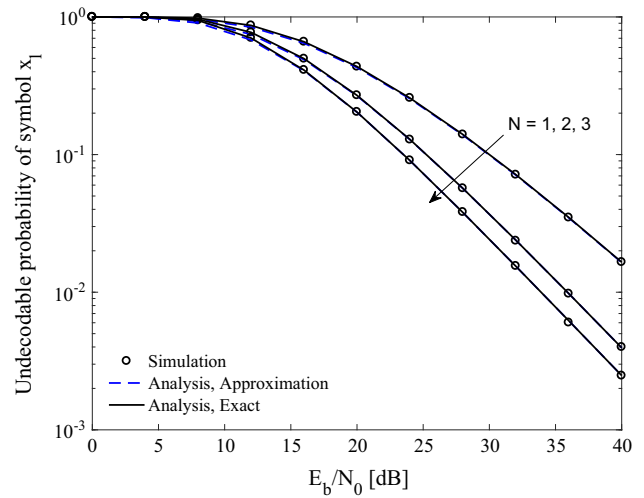


Fig. 2 Undecodable probability of x_1 for the perfect SIC and different number of the relay nodes, N

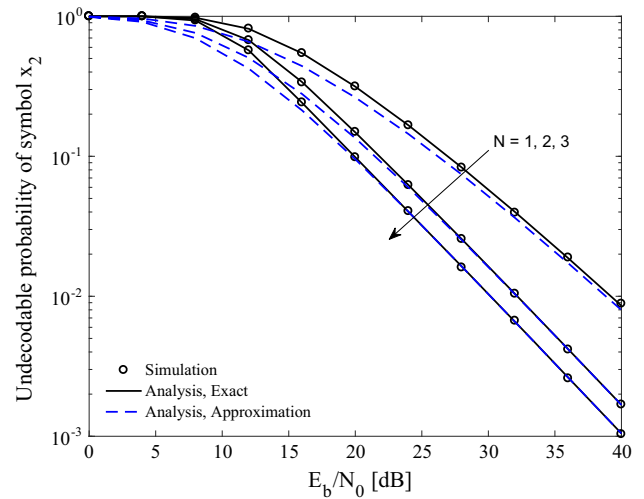


Fig. 3 Undecodable probability of x_2 for the perfect SIC and different number of the relay nodes, N

Let β and $(1 - \beta)$ Hz denote the bandwidth assigned for D_1 and the remaining bandwidth assigned for D_2 , respectively, where $(0 \leq \beta \leq 1)Hz$. By using Equ. (7.4) of [13], the sum capacity of the OMA system is given by

$$C_{OMA} = \frac{1-\alpha}{2} \beta \log_2 \left[1 + \min \left(\frac{P_S |h_1|^2}{\beta}, \frac{P_R |g_1|^2}{\beta} \right) \right] + \frac{(1-\alpha)(1-\beta)}{2} \log_2 \left[1 + \min \left(\frac{P_S |h_1|^2}{1-\beta}, \frac{P_R |g_2|^2}{1-\beta} \right) \right] \tag{49}$$

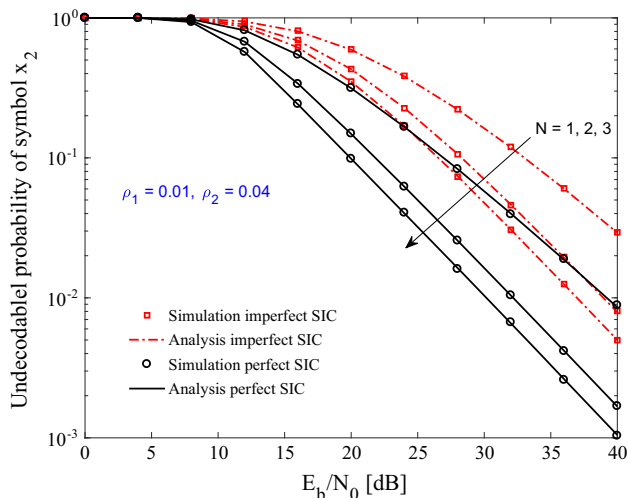


Fig. 4 Comparison of undecodable probability of x_2 for the perfect and imperfect SIC

4 Simulation results

In this section, several representative numerical results are provided to evaluate the impact of the number of relays, the channel gain (distance or path loss), and the imperfect SIC on the performance of NOMA systems with RF EH. The system parameters are as follows. The target data rates $r_1 = 0.5$ (bpcu) and $r_2 = 1$ (bpcu), the energy harvesting fraction $\alpha = 0.3$. The channel gains $\Omega_{SR_b} = \Omega_{R_bD_1} = 1$ and $\Omega_{R_bD_2} = 2$, and the energy conversion efficiency $\eta = 1$. The power allocation coefficient satisfies $\frac{\Omega_{R_bD_1}}{\Omega_{R_bD_2}} = \frac{a_2}{a_1}$ which is used to keep the trade-off between system throughput and user fairness.

Figures 2 and 3 plot the undecodable probability of symbols x_1 and x_2 , respectively for the case of perfect SIC.

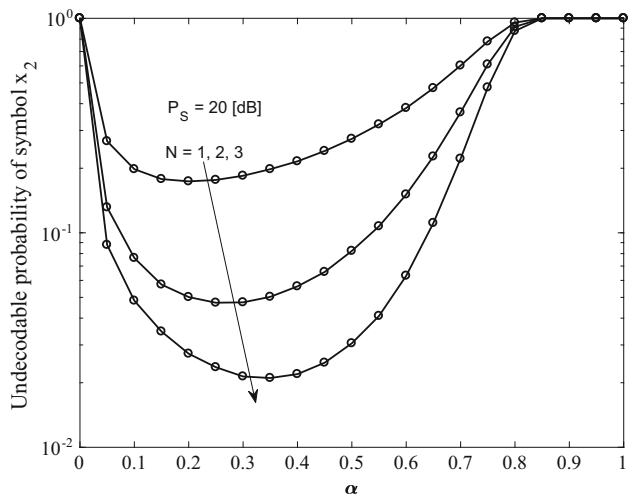


Fig. 5 Impact of fraction of block time, α , on the undecodable probability of symbol x_2

The result calculated by Eqs. (16) and (21) is named as Analysis-Exact, whereas the result calculated by using closed-form, Eqs. (17) and (22), is named as Analysis-Approximation. In this scenario, we consider the PRS scheme in which the number of relays is varied. It is recognized from Figs. 2 and 3 that the performance gain is increased by increasing the number of relays from 1 to 3. The reason is the selected best relay provides the best channel from the source to the relay in order to achieve better decoding performance as well as higher RF EH from the source in the first phase. We can see that the simulation results are in excellent agreement with the analytical results in all cases.

Figure 4 shows the comparison of the undecodable probability of x_2 versus the average SNR for the cases of perfect and imperfect SIC with the levels of residual interference, ρ , at the best relay and D_2 are $\rho_1 = 0.01$ and $\rho_2 = 0.04$, respectively. We should be reminded that D_1 should decode only symbol x_1 , while D_2 has to correctly decode x_1 first, and then use the SIC to obtain x_2 . The undecodable probability of symbol x_2 is plotted according to the average SNR in dB. The round and square markers indicate the simulation results of the perfect and the imperfect SIC, respectively. From Fig. 4, we can know that the remaining coefficient SIC significantly impacts the performance of D_2 . It is noticed that the simulation results are again in excellent agreement with the analytical results in all cases, which validates our mathematical models.

We also investigate the impact of fraction of block time, α , on the undecodable probability of symbol x_2 with different number of relay nodes, and depict the results in Fig. 5. In this scenario, we assume that the SIC is perfect and the transmit power from the source $P_S = 20$ dB. As shown in Fig. 5, there is the optimal α in the sense of

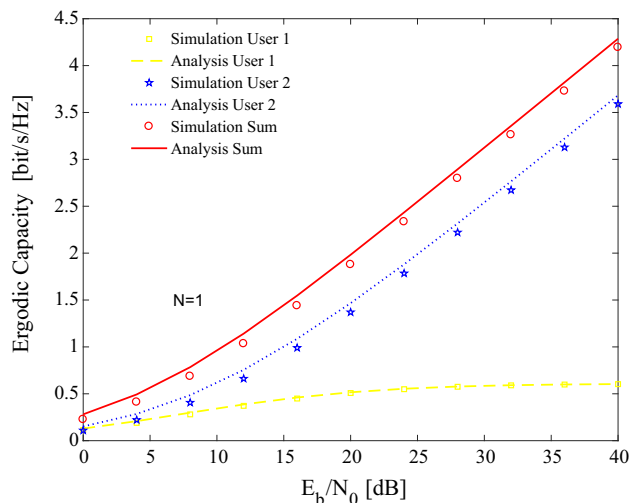


Fig. 6 Ergodic capacity versus SNR with number of relay nodes $N = 1$ and perfect SIC

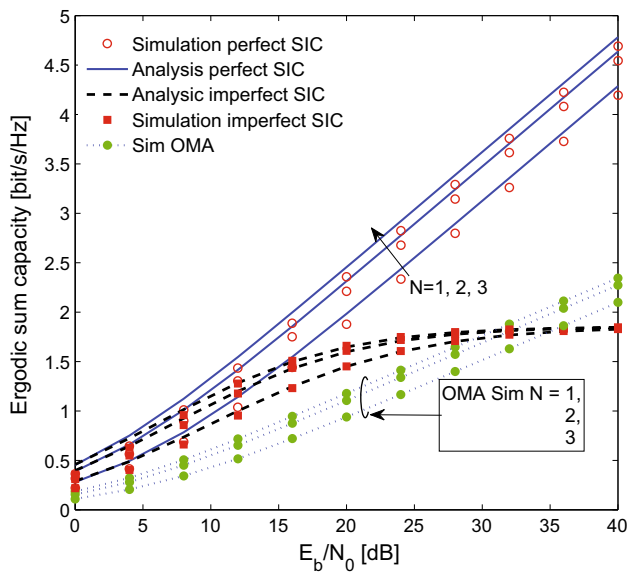


Fig. 7 Sum of ergodic capacity of two users with PRS scheme when the number of relays changes

minimal undecodable probability of symbol x_2 , and these minimal undecodable probabilities as well as the optimal α depend on the number of relay nodes, N . When N increases, the minimal undecodable probability becomes smaller while the optimal α becomes larger. The reason is, when N increases, the SINR of symbol x_2 , γ_{1u_2} , also increases because of the application of PRS. Thus, the data rate between the source and the best relay increases, and then the transmission time from the source to the best relay becomes shorter meaning the duration time for EH, α , is extended. With the larger α , the transmission power of the best relay is higher, and then the SINR of symbol x_2 at D_2 also becomes better. Consequently, according to (18), the undecodable probability of symbol x_2 decreases when the SINR of both the best relay and D_2 increases.

In Fig. 6, we plot the ergodic capacity of D_1 and D_2 versus E_b/N_0 . We can see that the analysis result of the ergodic capacity for D_1 matches excellently with the simulation result at the high SNR. The reason is that, we changed the instantaneous capacity of the information symbol x_1 from (30) into (31) under condition of the medium and high region power of the source. In addition, the upper bound curve of the ergodic capacity for D_2 and sum of the ergodic capacity for all users are close to the simulation results due to approximation of the CDF of the information symbol x_2 from (22).

In Fig. 7, the impact of the number of relay nodes on SWIPT-NOMA is depicted through the sum of ergodic capacity of D_1 and D_2 , for several number of relays, $N = 1, 2, 3$. We can understand that, the sum of ergodic capacity can be improved by setting up more number of

relays. However, the sum of ergodic capacity is just slightly improved when the number of relay nodes is high.

Compared with perfect SIC, the ergodic sum capacity of imperfect SIC is lower, and the gap of them increases when the E_b/N_0 increases. The reason is, while E_b/N_0 increasing, the interference term due to imperfect SIC increases, therefore the SINR as well as the ergodic capacity slowly increase.

The ergodic capacity of OMA-EH is also depicted in Fig. 7. For OMA, the equal power and equal bandwidth are applied for each user. As shown in Fig. 7, in case of perfect SIC, NOMA outperforms OMA because the SNR of OMA is higher than that of NOMA, however the bandwidth is just a half of NOMA and the capacity is linear with bandwidth. In case of imperfect SIC, the OMA outperforms NOMA when $\frac{E_b}{N_0}$ is high because of extremely decreasing of SINR of x_2

5 Conclusions

In this paper, we have analyzed the influence of EH technique in NOMA relay networks. The PRS scheme was applied to improve the system performance. The closed-form expression of the probability of unsuccessful decoding symbol x_1 , x_2 and ergodic capacity were derived. The theoretical analysis was verified by the Monte Carlo simulation method. From the theoretical and simulation results, some important conclusions can be summarized as follows. (1) The represented simulation results verified the correctness of our mathematical analysis. (2) The undecodable probability and the ergodic capacity were improved by increasing the number of relay nodes, however the large number of relay nodes is unnecessary for significantly improving the system performance. (3) There is the optimal duration time of EH for the minimal undecodable probability and it is directly proportional to the number of relay nodes. (4) The proposed system was analyzed in both perfect and imperfect SIC, and compared with OFDMA system, the impact of residual interference was discussed.

As future works, we will apply NOMA into multiple-relay multiple-antenna EH relay networks and analyze the network performance over Nakagami- m fading channel or double Rayleigh fading channel. In addition, we will investigate the impact of imperfect CSI on the performance of relay selection method.

Acknowledgements The authors would like to thanks Dr. Tran Trung Duy for his comment to improve quality of this page.

References

1. Wang, Y., Ren, B., Sun, S., Kang, S., & Yue, X. (2016). Analysis of non-orthogonal multiple access for 5G. *China Communications*, 13(Supplement 2), 52–66.
2. Dai, L., Wang, B., Yuan, Y., Han, S., Chih-Lin, I., & Wang, Z. (2015). Non-orthogonal multiple access for 5G: Solutions, challenges, opportunities, and future research trends. *IEEE Communications Magazine*, 53(9), 74–81.
3. Luo, S., & Teh, K. C. (2017). Adaptive transmission for cooperative NOMA system with buffer-aided relaying. *IEEE Communications Letters*, 21(4), 937–940.
4. Kader, M. F., Shahab, M. B., & Shin, S.-Y. (2017). Exploiting non-orthogonal multiple access in cooperative relay sharing”. *IEEE Communications Letters*, 21(5), 1159–1162.
5. Du, C., Chen, X., & Lei, L. (2017). Energy-efficient optimisation for secrecy wireless information and power transfer in massive MIMO relaying systems. *IET Communications*, 11(1), 10–16.
6. Sun, R., Wang, Y., Wang, X., & Zhang, Y. (2016). Transceiver design for cooperative non-orthogonal multiple access systems with wireless energy transfer. *IET Communications*, 10(15), 1947–1955.
7. Han, W., Ge, J., & Men, J. (2016). Performance analysis for NOMA energy harvesting relaying networks with transmit antenna selection and maximal-ratio combining over Nakagami-m fading. *IET Communications*, 10(18), 2687–2693.
8. Liu, Y., Ding, Z., Elkashlan, M., & Poor, H. V. (2016). Cooperative non-orthogonal multiple access with simultaneous wireless information and power transfer. *IEEE Journal on Selected Areas in Communications*, 34(4), 938–953.
9. Zwillinger, D. (2014). *Table of integrals, series, and products*. Amsterdam: Elsevier.
10. Pedersen, K. I., Kolding, T. E., Seskar, I., & Holtzman, J. M. (1996). Practical implementation of successive interference cancellation in DS/CDMA systems. In *IEEE international conference on universal personal communications, 1996. Record* (Vol. 1, pp. 321–325). IEEE
11. Gu, Y., & Aïssa, S. (2015). RF-based energy harvesting in decode-and-forward relaying systems: Ergodic and outage capacities. *IEEE Transactions on Wireless Communications*, 14(11), 6425–6434.
12. Michalopoulos, D. S., Suraweera, H. A., & Schober, R. (2015). Relay selection for simultaneous information transmission and wireless energy transfer: A tradeoff perspective. *IEEE Journal on Selected Areas in Communications*, 33(8), 1578–1594.
13. Benjebbour, A., Saito, K., Li, A., Kishiyama, Y., & Nakamura, T. (2016). Non-orthogonal multiple access (NOMA): Concept and design. In *Signal processing for 5G: Algorithms and implementations*, John Wiley and Sons (Chap. 7, pp. 143–168)
14. Yang, Z., Ding, Z., Fan, P., & Al-Dhahir, N. (2017). The impact of power allocation on cooperative non-orthogonal multiple access networks with swipt. *IEEE Transactions on Wireless Communications*, 16(7), 4332–4343.
15. Papoulis, A., & Pillai, S. U. (2002). *Probability, random variables, and stochastic processes*. New York City: Tata McGraw-Hill Education.



Tran Manh Hoang was born on 07/11/1977. He is received the B.S. degree in Communication Command at Telecommunications University, Ministry of Defense, Vietnam, in 2002, and the B.E. degree in Electrical Engineering from Le Quy Don Technical University, Ha Noi, Vietnam, in 2006. He obtained the M.E. degree in Electronics Engineering from Posts and Telecommunications, Institute of Technology, (VNPT), Vietnam, in 2013. He is currently pursuing the Ph.D. degree at Le Quy Don Technical University, Hanoi, Vietnam. His research interests include energy harvesting, Non-orthogonal Multiple Access, and signal processing for wireless cooperative communications.



Nguyen Trung Tan was born in Ha Nam, Viet Nam. He received the B.S. in 2004 and M.S. in 2007 in Electrical Engineering from Le Quy Don Technical University, Ha Noi, Vietnam. He subsequently received the Ph.D. degree in 2013 in Electrical Engineering from Harbin Institute of Technology, China. After his Ph.D., he worked at Center for Telecommunication Engineering, Le Quy Don Technical University, Vietnam. His research interests lie within the areas of wireless communication, cooperative communication, cognitive radio.



Nguyen Huy Hoang received B.E., M.E. and Ph.D. degree in Electronic Engineering from Le Quy Don Technical University, Vietnam, in 1986, 1997 and 2007, respectively. He is currently lecturer at Le Quy Don Technical University, Vietnam. His research concentrates on the area of wireless information, communication technologies, microwave electronic circuit.



Pham Thanh Hiep received the B.E. degree in Communications Engineering from National Defence Academy, Japan, in 2005; received the M.E. and Ph.D. degree in Physics, Electrical and Computer Engineering from Yokohama National University, Japan, in 2009 and 2012, respectively. He was working as associate researcher at Yokohama National University, Yokohama, Japan from 2012 to 2015. Now, he is a lecturer at Le Quy Don

Technical University, Ha Noi, Viet Nam. His research interests lie in the area of wireless information and communications technologies.